Diffusion Through the Liquid-Liquid Interface

W. J. WARD and J. A. QUINN

University of Illinois, Urbana, Illinois

Several mechanisms have been proposed for the process of interphase mass transfer (*8*). Of these models the two most widely applied have been the so-called *film theory* and the more physically plausible *penetration theory*. Both models assume that chemical equilibrium exists at the interface and therefore that the interface itself offers no resistance to the transfer. In several recent studies a variety of techniques have been used to measure the departure from equilibrium or an interfacial resistance (*6, 11, 16, 18*). In particular, studies on the gas-liquid interface indicate that for slightly soluble gases, such as carbon dioxide in water, a state indiscernible from equilibrium is attained at a freshly-formed liquid surface within times of the order of a millisecond (*10, 11, 13, 16*). For such systems any interfacial resistance is vanishingly small. However for the system oxygen-water a measurable resistance has been reported (*5*). For the liquid-liquid interface widely conflicting results have been reported (*3, 8, 9, 17, 18*) extending from claims of no resistance up to resistances of the order of 10^3 to 10^6 sec./cm.

Much of the apparent contradiction in the liquid-liquid area is due to an incomplete knowledge of the physicochemical and hydrodynamic factors which are present in these experiments. Most work on liquid-liquid transfer has been carried out with static systems (*8, 18*), with the obvious disadvantage that long contact times are involved. With static systems the bulk-phase resistances are controlling, and interfacial resistances smaller than 10^3 sec./cm. are difficult to detect. Also with static systems one is more likely to encounter the so-called *Marangoni effects*, and interface contamination is a more serious problem.

From these considerations it appears that a dynamic experiment with a small contact time is necessary in studying transfer through the liquid-liquid interface. In the last 2 yr. dynamic experiments on two-component liquid-liquid systems have been reported by Ratcliff and Reid (*15*) and by Quinn and Jeannin (*12*). Ratcliff and Reid measured the diffusivity of benzene in water with a spherical-film absorber similar to the apparatus used by Davidson and Cullen (*7*) in gas-liquid studies. Their results, with nominal contact times as small as 0.5 sec., agreed well with theory and showed no signs of an interfacial resistance for benzene transferring into water. Jeannin employed a laminar liquid-liquid jet, and at contact times of 0.05 sec. to 0.5 sec. he detected what appeared to be an interfacial resistance of approximately 80 sec./cm. for isobutanol diffusing into water.

The interpretation of the above experiments, as well as all dynamic mass transfer studies, calls for a detailed knowledge of the flow field close to the interface. It appears that Ratcliff and Reid were successful in analyzing the velocity field for the laminar film flowing over the sphere; there is however some question as to the acceleration of the laminar jet in the work of Jeannin. Both techniques are suitable only for two-component systems or possibly three-component systems where the bulk-phase resistance in one liquid is small.

In the present investigation measurements have been made on the systems benzene-water and toluene-water with a laminar jet apparatus wherein one phase is spread as a thin film on the surface of a laminar jet. With the apparatus described below it is possible to contact two liquid phases for times as small as 0.01 sec. Thus bulk-phase resistances are small, and it is therefore possible to detect small departures from equilibrium at the interface. The method is suitable for studies on three-component systems, and as reported here the technique can be used to measure precise values of liquid diffusivities.

EXPERIMENTAL

A flow diagram of the apparatus is shown in Figure 1. Demineralized, de-aerated water was fed from a reservoir to a constant temperature bath maintained at 25°C. and then to a constant head device. Flow rate was controlled with a Teflon stopcock in the line immediately upstream from the nozzle. The organic phase was delivered similarly through an all-glass line. At two points in the glass line it was necessary to have flexible joints. This was accomplished by butting the ends of the glass tubing together and placing a short length of Tygon tubing over the joint. Other than these joints the only materials which the liquids contacted were glass, Teflon, and stainless steel.

The jet chamber was a 4.5 in. length of 3 in. I.D. Pyrex pipe clamped between stainless steel flanges. The chamber was sealed to the flanges with Teflon gaskets. The bottom flange was bolted to a massive platform resting on a rubber mat.

A sketch of the nozzle apparatus and receiver is shown in Figure 2. The entire nozzle apparatus was constructed of stainless steel. The organic liquid flowed onto the water jet from the small annular opening (approximately 0.01 cm. in width) above the tip of the water nozzle. The receiver was a 9 in. length of 0.2 cm. I.D. precision bore glass tubing. The inner lip of the receiver was slightly countersunk, and the outer edge was tapered with a flat portion between the countersink and taper. The receiver was forced through a tight-fitting Teflon

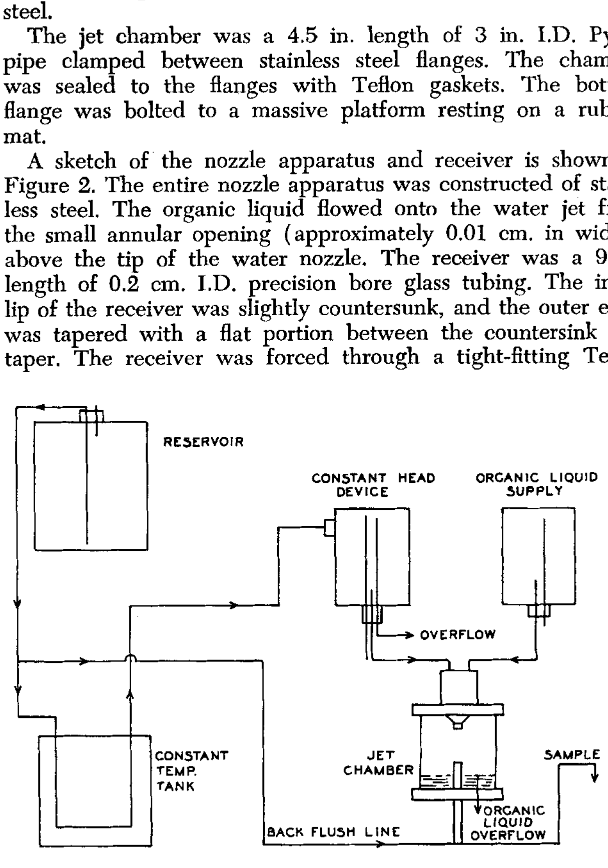

Fig. 1. Flow diagram.

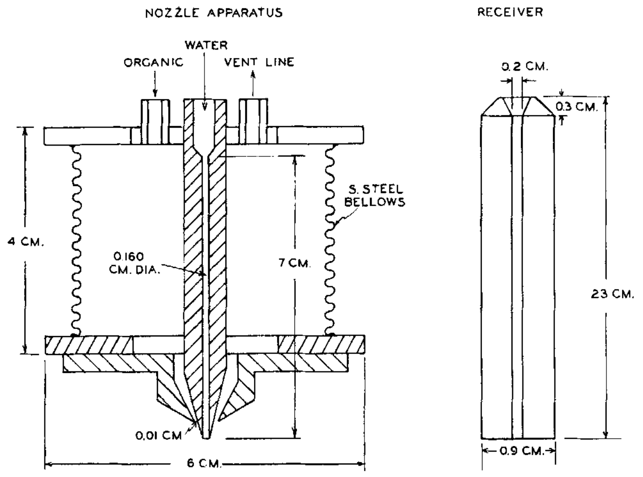

Fig. 2. Nozzle apparatus and receiver.

bushing in the bottom plate. By adjusting the level of the receiver the desired jet lengths could be obtained. The jet lengths and profiles were measured with a cathetometer fitted with a traveling microscope.

OPERATION

In making a run the first step was to start the organic liquid flowing with the sample line filled with water and closed. With the vent line of the nozzle apparatus open, the bellows section was completely filled with the organic phase. Next the vent line was closed and the organic liquid flow rate set at approximately 1.5 cc./min. The water was then turned on, and the jet was centered on the receiver.

The level of the outlet of the sample line, which was adjusted by means of a geared device attached to the line, was set at its maximum height, and the valve on the sample line was opened. At this point all of the organic liquid spilled over and down the outside of the receiver. The level of the sample line was carefully lowered to the point at which the jet was exactly balanced; that is all of the organic liquid spilled over the outside of the receiver and all of the water passed into the receiver. It was not difficult to determine the exact balance point. If it were slightly overbalanced, a large drop of water slowly built up on the tip of the receiver and then suddenly fell off and ran down the outside of the receiver. If the jet were under balanced, the drops of organic liquid in the receiver and sample line were clearly visible. If during a run the jet became under balanced, the sample line was replaced and the receiver was thoroughly flushed with water from the backwash line. The fact that the jet was exactly balanced during operation is further confirmed by the reproducibility and consistency of the mass transfer data obtained.

The water flow rate was measured by collecting the effluent over a timed interval. The flow rate did not vary by a measurable amount (0.5%) over the period of a run. The organic liquid flow rate was measured by collecting the effluent from the chamber.

Because the organic liquids were highly volatile and bulk concentrations were small, several precautions were taken in handling the samples. Samples were collected in modified screw-cap glass vials of 3 cc. capacity. It was necessary that the vials be completely filled and air tight to prevent loss of the organic by evaporation. Teflon disks, 1/16 in. thick, were fitted into the caps and the vials were sealed while the liquid from the sample line was overflowing the vials.

CHEMICAL ANALYSIS

A gas chromatograph equipped with hydrogen flame detector was used to measure the extremely small concentrations of benzene and toluene in water. A recorder with a disk integrator was used in conjunction with the chromatography units. Ten microliter samples were withdrawn from the sample vials and injected into the chromatograph with a syringe.

Successful techniques were developed for calibrating peak area vs. concentration and for measuring the solubilities of benzene and toluene in water (*19*). Widely varying solubilities have been reported for both benzene and toluene in water. The values obtained here for the saturation concentrations at 25°C. are:

Benzene in water:	2.23×10^{-5} g.moles/cc.
Toluene in water:	6.01×10^{-6} g.moles/cc.

The value for benzene is the same as that reported by Arnold, et al. (*2*). The value for toluene is intermediate between the results of Andrews and Keefer (*1*) and Bohn and Claussen (*4*).

DIFFUSION CALCULATIONS

In this experiment the directly measurable quantities were average concentration of solute in the aqueous stream, volumetric flow rate, length of jet, and diameter of the jet at points downstream from the nozzle. A method is described below for proceeding from these measured quantities to an interpretation of the mass transfer process.

It is assumed throughout that the outer skin of organic fluid does not affect the flow within the water jet. (Typical flow rates for the core and skin were 60 and 1.5 cc./min., respectively, with the thickness of the outer phase everywhere less than 10 μ.) The problem of absorption into a laminar jet witth negligible surface drag has been treated by Scriven and Pigford (*16*). Their solution for the local rate of mass transfer into the jet is

$$N = (C^* - C_o)\sqrt{\frac{D}{\pi}\,\frac{u_s^2}{\int_0^x u_s\,dx}} \qquad (1)$$

The principal assumptions in the derivation of Equation (1) are: (1) interfacial equilibrium; (2) for the diffusing molecules the jet is effectively semi-infinite; (3) with zero drag at the surface the axial velocity is equal to the surface velocity, u_s, over the depth of penetration.

For an ideal jet, one in which the velocity is everywhere constant, Equation (1) becomes

$$N_i = (C^* - C_o)\sqrt{\frac{D\,u_o}{\pi\,x}} \qquad (2)$$

with

$$u_o = \frac{Q}{\pi R_o^2} \qquad (3)$$

Integration over the surface of the jet gives the average concentration

$$\overline{C} - C_o = \frac{1}{Q}\int_o^x 2\pi R(x)N(x)\,dx \qquad (4)$$

and for the ideal jet

$$\overline{C_i} - C_o = 4\,(C^* - C_o)\sqrt{\frac{Dx}{Q}} \qquad (5)$$

Thus for an ideal jet a plot of $(\overline{C} - C_o)/(C^* - C_o)$ vs. $\sqrt{x/Q}$ would be a straight line passing through the origin with slope $4\sqrt{D}$. It is convenient to compare experimental data with Equation (5) and to examine the departure from ideality of the actual jet.

For a plot of $(\overline{C} - C_o)/(C^* - C_o)$ vs. $\sqrt{x/Q}$ the slope S predicted from Equations (1) and (4) is

$$S = 4\sqrt{D}\left\{\frac{\pi R^2}{Q}\,\frac{u_s^2 x}{\int_o^x u_s\,dx}\right\}^{1/2} \qquad (6)$$

Therefore the ratio of the actual to the ideal slope becomes

$$\frac{S}{S_i} = \left\{ \frac{u_s}{\bar{u}} \frac{u_s x}{\int_0^x u_s\, dx} \right\}^{1/2} \tag{7}$$

with

$$\bar{u} = \frac{Q}{\pi R^2} \tag{8}$$

At this point certain features of the experimental curve can be predicted. First consider Equation (7) as x approaches zero:

$$u_s(0) = 0 \text{ and } \bar{u}(0) \neq 0$$

Therefore

$$\lim_{x \to 0} \frac{S}{S_i} = 0 \tag{9}$$

Similarly as x becomes large the velocity in the jet is uniform, and u_s becomes equal to $\bar{u}$. Furthermore for large x the velocity in the jet can be calculated from gravitational effects alone (*15*), and

$$\lim_{x \to \infty} \frac{du_s}{dx} = 0$$

Therefore

$$\lim_{x \to \infty} \frac{S}{S_i} = 1 \tag{10}$$

Thus a plot of $(\bar{C} - C_o)/(C^* - C_o)$ vs. $\sqrt{x/Q}$ has zero slope at the origin, and the slope approaches $4\sqrt{D}$ at large values of x. Depending on the diameter profile, as explained below, the slope at intermediate points may be greater or less than $4\sqrt{D}$.

More specific knowledge of the surface velocity of the jet is necessary if experiment is to be compared with theory. At the nozzle $u_s = 0$, and at any point beyond the nozzle u_s has a finite value. The simplest expression which satisfies these conditions is an equation of the form

$$u_s = ax^n, \; 0 < n < 1 \tag{11}$$

With this assumption for the surface velocity Equation (7) becomes

$$\frac{S}{S_i} = \left\{ \frac{(n+1)\, ax^n}{\bar{u}} \right\}^{1/2} \tag{12}$$

At some point x_1 down from the nozzle the surface velocity is equal to the average velocity; that is the flow is uniform across the jet:

$$u_s(x_1) = \bar{u}(x_1) \tag{13}$$

Assume that at this point

$$\left.\frac{du_s}{dx}\right|_{x_1} = \left.\frac{d\bar{u}}{dx}\right|_{x_1} \tag{14}$$

Equations (8), (12), (13), and (14) combine to give

$$\left.\frac{S}{S_i}\right|_{x_1} = \left\{ 1 - \left(\frac{2x}{R} \frac{dR}{dx} \right)_{x_1} \right\}^{1/2} \tag{15}$$

In order to use Equation (15) it is necessary to know the point at which the flow is essentially uniform. Assuming that the surrounding air exerts negligible drag on the jet, neglecting surface effects, and assuming that the pressure within the jet is uniform throughout, an overall momentum balance between the nozzle and a point downstream is

$$\int_0^{R(x)} 2\pi r \rho u^2 dr = \int_0^{R_o} 2\pi r \rho u_o^2 dr + \int_0^x \pi R^2 \rho g dx \tag{16}$$

With fully developed laminar flow in the nozzle Equation (16) can be rearranged for points greater than x_1 to

$$\frac{4}{3} = \left(\frac{R_o}{R} \right)^2 - \frac{\pi^2 g R_o^4}{Q^2} \int_0^x \left(\frac{R}{R_o} \right)^2 dx, \; x \geqq x_1 \tag{17}$$

Plotting the right hand side of Equation (17) vs. x one should get a smooth curve which approaches a value of 4/3. The value of x at which this occurs is then the point at which the flow is essentially uniform ($x = x_1$).

Equation (15) can be simplified by evaluating dR/dx from Equation (16). In final form then

$$\left.\frac{S}{S_i}\right|_{x_1} = \left\{ 1 + \frac{gx}{\bar{u}_o^2} \left(\frac{R}{R_o} \right)^4 \right\}^{1/2}_{x_1} \tag{18}$$

As a check on the measured profiles upper and lower bounds for the radius of the jet can be obtained from Equation (16). For a jet falling under gravity (*15*) the maximum radius corresponds to a jet having a flat velocity profile at the nozzle and at all downstream points. With the assumption of a one-dimensional flow (even though the jet is gradually contracting) the maximum profile is approximated by

$$\frac{R}{R_o} < [1 + \beta]^{-1/4}, \; \beta = \frac{2gx}{\bar{u}_o^2} \tag{19}$$

For a jet with initial parabolic profile and with the above inequality used to evaluate the gravitational term of Equation (16) a minimum profile is obtained:

$$\frac{R}{R_o} > \left[\frac{1}{3} + \sqrt{1 + \beta} \right]^{-1/2} \tag{20}$$

RESULTS AND DISCUSSION

The experimental results for the diffusion of benzene and toluene into water at 25°C. are shown in Figures 3 and 4. The results are plotted with average concentration as a function of jet length and flow rate, $\bar{C}/C^*$ vs. $\sqrt{L/Q}$. The benzene-water runs were made at jet lengths between 2 and 8 cm. and water flow rates of 0.7 to 2.2 cc./sec. The toluene-water measurements were carried out with jet lengths of 2, 4, and 6 cm. with water flow rates of 1.01 and 1.67 cc./sec.

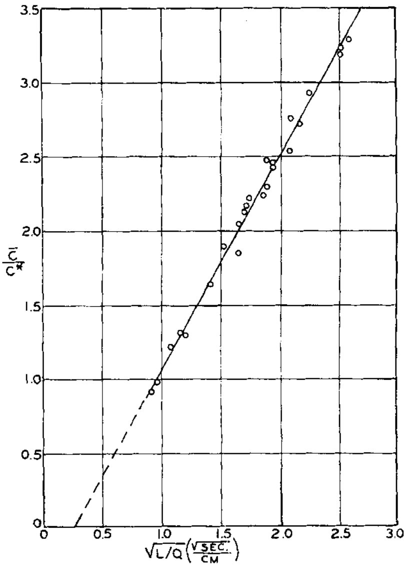

Fig. 3. $\overline{C}/C^*$ vs. $\sqrt{L/Q}$, benzene-water system at 25°C.

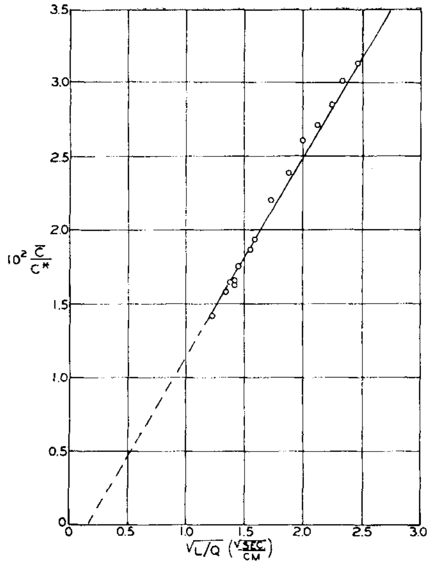

Fig. 4. $\bar{C}/C^*$ **vs.** $\sqrt{L/Q}$**, toluene-water system at 25°C.**

For the benzene-water system the spread in concentration within any given run was less than 4%. The average standard deviation within a run was 0.05×10^{-7} moles/cc., and the range of concentrations covered was from 2.04 to 7.31×10^{-7} moles/cc. For the toluene-water system the percentage spread in concentration within a run was comparable to the results with benzene. The average standard deviation within each run was 0.007×10^{-7} moles/cc., while the range in concentration covered was from 0.852×10^{-7} to 1.892×10^{-7} moles/cc.

The experimental points in Figures 3 and 4 were fitted by a least-squares analysis. The equations of the resulting lines (indicated as solid lines in Figures 3 and 4) are

Benzene-water at 25°C.

$$\bar{C}/C^* = 0.0145\sqrt{L/Q} - 0.0039$$

Toluene-water at 25°C.

$$\bar{C}/C^* = 0.0136\sqrt{L/Q} - 0.0021$$

For benzene all experimental points are within 6% of the fitted line, and for toluene all points are within 5%.

Jet diameter measurements for water flow rates of 1.01 cc./sec. and 1.67 cc./sec. are shown in Figure 5.

The data of Figures 3 and 4 extrapolate to an intercept on the abscissa of approximately 0.2 $\sqrt{\text{sec.}}$/cm. For two is led to expect an intercept. First, as shown by Equation reasons, both a result of the fluid dynamics of the jet, one (9), the ratio of the actual to the ideal slope must approach zero at the origin. Second, S/S_i is greater than 1 over the range of flow rates and jet lengths covered in the experiment. These two features of the curve indicate that if a straight line is drawn through data which are sufficiently removed from the origin the fitted line will have a positive intercept on the abscissa.

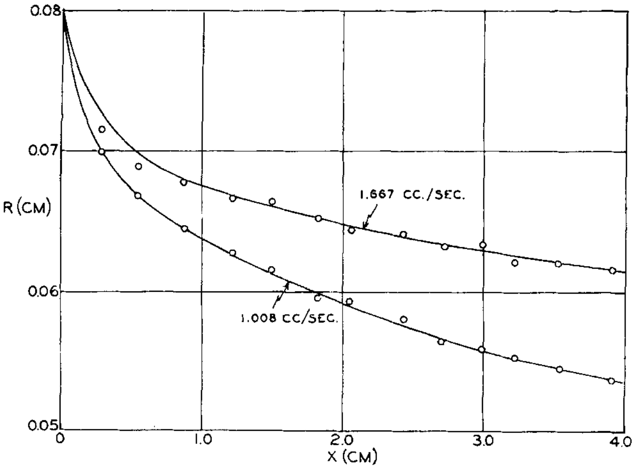

Fig. 5. Jet profiles at 1.667 and 1.008 cc./sec.

An intercept on the abscissa is also to be expected if there is an appreciable resistance to mass transfer at the interface. Neglecting the fluid mechanical effects and assuming that the intercept is solely the result of a resistance (which is not correct for reasons stated above) one can calculate an upper limit for the interfacial resistance.

For an ideal jet with interfacial mass transfer coefficient k_s the average concentration as a function of contact time is given by (*10*):

$$\frac{\bar{C}-C_o}{C^*-C_o}=\frac{4}{d}\left\{2\sqrt{\frac{Dt}{\pi}}+\frac{D}{k_s}\left[\frac{1}{k_s}\sqrt{\frac{D}{\pi t}}-1\right]\right\} \tag{21}$$

The intercept of Figures 3 and 4 corresponds to a contact time of approximately 0.001 sec. For this intercept Equation (21) gives k_s as 0.09 cm./sec. or an interfacial resistance of 11 sec./cm. Therefore it can be concluded that if there is an interfacial resistance to the transfer of benzene or toluene to water, the resistance is less than 11 sec./cm.

As a check on the analysis of the diffusional process, values of the diffusivity of benzene and toluene in water can be calculated from the slopes of the experimental curves from Equation (18). The point at which the velocity in the jet became uniform, x_1, was determined from Equation (17). The calculation of x_1 is somewhat arbitrary in that x_1 is taken as that value of x at which the right-hand side of Equation (17) is equal to 4/3. Since the value 4/3 is approached asymptotically, it is difficult to assign a precise value to x_1. The calculations indicated a value of x_1 between 1.5 and 2.5 cm. for a flow rate of 1.01 cc./sec. and 2.0 to 3.0 cm. for a flow rate of 1.67 cc./sec. The best value of x_1 is probably midway between the values listed above. The calculated diffusivities are listed in Table 1.

The spread in the diffusivity values is approximately 11%, with the ratio of the diffusivity of benzene to that of toluene equal to 1.13.

Since the average of the experimental values for the diffusivity differs for the two flow rates by approximately 8%, the data on the plot of $\bar{C}/C^*$ vs. $\sqrt{L/Q}$ should fall on distinct lines depending on the flow rate. However the difference in the slopes of these lines (4%) is within the experimental error, and distinct lines are not discerned. One line has been drawn through the data for each system, and the best estimate for the diffusivity is taken as the average of the values calculated at each flow rate.

TABLE 1. CALCULATED VALUES OF DIFFUSIVITY

Flow rate, cc./sec.	Assumed value of x_1, cm.	D for benzene in water, 25°C., sq. cm./sec. × 10^5	D for toluene in water, 25°C., sq. cm./sec. × 10^5
1.67	2.0	1.16	1.03
1.67	2.5	1.14	1.01
1.67	3.0	1.12	0.992
1.01	1.5	1.07	0.965
1.01	2.0	1.06	0.938
1.01	2.5	1.04	0.920
		Average 1.10	0.975

TABLE 2. DIFFUSIVITY OF BENZENE AND TOLUENE IN WATER AT 25°C.

	Benzene $D \times 10^5$, sq. cm./sec.	Toluene $D \times 10^5$, sq. cm./sec.
Empirical correlation of Wilke and Chang (*14*)	1.09	0.961
Empirical correlation of Othmer and Thakar (*14*)	1.02	0.905
Experimental results of Ratcliff and Reid (*15*)	1.14 (liquid) 1.09 (vapor)	
Authors	1.10	0.975

As mentioned above the runs with benzene were carried out over a range of flow rates from 0.7 to 2.5 cc./sec. The diffusivity of benzene in water was calculated from jet profiles measured at 1.01 and 1.67 cc./sec. These flow rates were assumed to be representative of the higher and lower flow rates actually used. This procedure is not exact, but the error introduced is small.

Diffusivities calculated from empirical formulas (*14*) and the experimental value for the diffusivity of benzene in water reported by Ratcliff and Reid are compared with the present measurements in Table 2. It is significant that the ratio of the diffusivity of benzene to toluene as predicted by both of the above correlations is 1.13, identical to the experimentally determined ratio. For two such similar compounds the correlations can be expected to predict accurate ratios of the diffusivities. Also it is reasonable to expect the experimental results to yield the correct ratio. The fluid dynamics for both systems are the same, and the ratio of the diffusivities is obtained by simply squaring the ratio of the slopes of the experimental lines on the plot of C/C^* vs. $\sqrt{L/Q}$. Errors introduced in the analysis leading to absolute values of D are not present in the calculation of the ratio of diffusivities.

Ratcliff and Reid (*14*) measured the diffusivity of benzene in water with benzene transferring to water from both the liquid and vapor phases. The values they have reported for the two cases are listed in Table 2. Measurements in the present work cover a wider range of contact times, and the times are an order of magnitude smaller than those attained by Ratcliff and Reid. The diffusivity values from the work of Ratcliff and Reid are in excellent agreement with those reported here.

Diffusivities were also calculated from Equation (18) with the upper and lower bounds for the radii of the jet predicted from Equations (19) and (20). The spread in values is roughly twice the range shown in Table 1 for diffusivities calculated from tthe experimental profile. The average diffusivities calculated by the two methods agree closely with values of 1.08 and 0.955 × 10^{-5} sq. cm./sec. as the average for benzene and toluene calculated from the predicted profiles.

ACKNOWLEDGMENT

Acknowledgment is made to the donors of the Petroleum Research Fund, administered by the American Chemical Society, for partial support of this research. A fellowship received by W. J. Ward from the Monsanto Chemical Company is also gratefully acknowledged.

NOTATION

a = constant, defined by Equation (11)
$\overline{C}$ = average concentration, g.-moles/cc.
$\overline{C_i}$ = average concentration in an ideal jet, g.-moles/cc.
C^* = equilibrium concentration, g.-moles/cc.
C_o = initial concentration, g.-moles/cc.
d = diameter of the jet, cm.
D = diffusivity, sq. cm./sec.
g = acceleration of gravity, cm./sec. sq.
k_s = interfacial mass transfer coefficient, cm./sec.
L = length of jet, cm.
N = local absorption rate, g.-moles/sq. cm.-sec.
N_i = local absorption rate of an ideal jet, g.-moles/sq. cm.-sec.
n = constant, defined by Equation (11)
Q = flow rate, cc./sec.
R = radius of the jet, cm.
R_o = initial radius of the jet, cm.
r = radial distance measured from the center of the jet, cm.
S = slope of the plot of $\overline{C}/C^*$ vs. $\sqrt{L/Q}$, cm./sec.$^{1/2}$
S_i = slope of the plot of $\overline{C}/C^*$ vs. $\sqrt{L/Q}$ for an ideal jet, cm./sec.$^{1/2}$
t = contact time, sec.
u = velocity in the axial direction, cm./sec.
u_s = surface velocity, cm./sec.
u_o = velocity in the axial direction at the nozzle, cm./sec.
$\overline{u}$ = average velocity, cm./sec.
x = coordinate axis
x_1 = distance down from the nozzle at which the surface velocity is equal to the average velocity, cm.
β = defined by Equation (19)
ρ = density, g./cc.

LITERATURE CITED

1. Andrews, L. J., and R. M. Keefer, *J. Am. Chem. Soc.*, **71**, 3645 (1949).
2. Arnold, D. S., C. A. Plank, E. E. Erickson, and F. P. Pike, *Chem. and Eng. Data Ser.*, **6**, 253, (1958).
3. Blokker, P. C., "Proceedings Second International Congress Surface Activity," vol. 1, p. 503, Academic Press, New York (1957).
4. Bohn, R. L., and W. F. Claussen, *J. Am. Chem. Soc.*, **73**, 1571 (1951).
5. Chiang, S. H., and H. L. Toor, *A.I.Ch.E. Journal*, **5**, 165 (1959).
6. Danckwerts, P. V., and A. M. Kennedy, *Chem. Eng. Sci.*, **8**, 201 (1958).
7. Davidson, J. F., and E. J. Cullen, *Trans. Inst. Chem. Engrs. (London)*, **35**, 51 (1957).
8. Davies, J. T., and E. K. Rideal, "Interfacial Phenomena," Academic Press, New York (1961).
9. Davies, J. T., and J. B. Wiggill, *Proc. Roy. Soc. London*, **A225**, 277 (1960).
10. Govindan, T. S., and J. A. Quinn, *A.I.Ch.E. Journal*, **10**, No. 1, p. 35 (1964).
11. Harvey, E. A., and W. Smith, *Chem. Eng. Sci.*, **10**, 274 (1959).
12. Quinn, J. A., and P. G. Jeannin, *ibid.*, **15**, 243 (1961).
13. Raimondi, P., and H. L. Toor, *A.I.Ch.E. Journal*, **5**, 86 (1959).
14. Reid, R. C., and T. K. Sherwood, "The Properties of Gases and Liquids," McGraw Hill, New York (1958).
15. Ratcliff, G. A., and K. J. Reid, *Trans. Inst. Chem. Engrs. (London)*, **39**, 423 (1961).
16. Scriven, L. E., and R. L. Pigford, *A.I.Ch.E. Journal*, **5**, 397 (1959).
17. Sinfelt, J. H., and H. G. Drickamer, *J. Chem. Phys.*, **23**, 1095 (1955).
18. Vignes, A., *J. de Chemie Physique*, **57** (1960).
19. Ward, W. J., M.S. thesis, University of Illinois, Urbana, Illinois (1963).

Manuscript received March 28, 1963; revision received July 10, 1963; paper accepted July 15, 1963.